Astron. Astrophys. 346, L53–L56 (1999)

ASTRONOMY AND ASTROPHYSICS

LETTER

Letter to the Editor

X-ray and radio evidence on the origin of a coronal shock wave

Karl-Ludwig Klein[1], **Josef I. Khan**[2,⋆], **Nicole Vilmer**[1], **Jean-Marc Delouis**[1], **and Henry Aurass**[3]

[1] Observatoire de Paris, Section de Meudon, DASOP, CNRS-UMR 8645, F-92195 Meudon, France
[2] Mullard Space Science Laboratory, University College London, Holmbury Saint Mary, Dorking, Surrey, RH5 6NT, UK
[3] Astrophysikalisches Institut Potsdam, Observatorium für solare Radioastronomie, An der Sternwarte 16, D-14482 Potsdam, Germany

Received 22 April 1999 / Accepted 18 May 1999

Abstract. Large-scale shock waves in the solar corona are observed through their characteristic radio emission at decimetric and longer wavelengths ("type II bursts"). Their driver has not been identified so far. Particularly favorable observing conditions on 27 November 1997 allowed us to combine imaging and spectroscopic observations of the shock signature over a broad radio band with X-ray imaging of plasma structures at high time resolution. The data provide evidence that the shock is generated by rapidly expanding or disrupting structures in the outskirts of the flaring active region: (1) the type II emission starts above the top of a pre-existing, highly inclined loop system at the time when a plasma blob ejected along the legs reaches the top; (2) the alignment of type II source positions at successively lower frequencies is far from radial with respect to the associated flare, but seems to be related to the orientation of the pre-existing loop system and the motion of the plasma blob.

Key words: shock waves – Sun: activity – Sun: corona – Sun: flares – Sun: radio radiation – Sun: X-rays, gamma rays

1. Introduction

Type II bursts at decimetric to dekametric wavelengths are radio signatures of extended shock waves in the solar corona (cf. reviews by Nelson & Melrose 1985; Mann 1995; Aurass 1997). Their origin may be either the sustained propagation at supermagnetosonic speeds of coronal material or a blast wave, i.e. a fast MHD shock generated by short localized energy release during a flare (e.g. Dryer 1981; Hundhausen 1985; Steinolfson 1985). Observations suggest that the type II shock in the low and middle corona results from processes during a flare, rather than being the bow shock of a coronal mass ejection (CME). Direct evidence for the flare association is given by the recent finding that type II precursor signatures occur from the onset of the impulsive flare in active region loops (Klassen et al. 1999). Arguments against the idea that decimetric-to-dekametric type II emission comes from the bow shock of a CME are provided both by statistical analyses and by studies of individual events: The few available imaging observations show that generally the type II source does not have the appropriate position or speed consistent with the bow shock of the white-light CME (Wagner & MacQueen 1983, Gopalswamy & Kundu 1995, and references therein; Klein et al. 1997; cf. Dryer 1982 for the discussion of counterexamples). Furthermore, a systematic study from metric to hectometric wavelengths during a period of weak activity (Gopalswamy et al. 1998) showed that type II bursts originating in the low corona fade before reaching interplanetary space. Arguing that at least some of the type II bursts should continue to long wavelengths if CMEs were the drivers, these authors attributed low (i.e., near surface) coronal type II emission to a blast wave in the flaring active region, on much smaller spatial scales than the CME.

Although the arguments that the CME is not the driver of the type II shock are to a certain extent circumstantial, the prevailing view is presently that type II emission in the low and middle corona is related to the flare, not to the CME. The question is then which specific process during a flare generates the type II shock. The identification of the region where the type II emission first arises and its relationship with the flaring active region structures is fundamental. This information is difficult to obtain: on the one hand the reliable identification of the shock wave requires spectrography and imaging in the same radio waveband. On the other hand, X-ray imaging at a cadence of a few tens of seconds is necessary to track the evolution of active region structures which may reveal the driver. Such structures have typical heights of (10^4-10^5) km, and in order to generate fast shocks, speeds of several (10^2-10^3) km s^{-1} must be reached. These combined observational requirements have not been met before.

On 27 November 1997 a bright type II burst was observed from decimetric to dekametric waves by the Tremsdorf spectrograph (Mann et al. 1992) and the Nançay Radioheliograph (henceforth NRH; Kerdraon & Delouis 1997), and soft and hard X-ray observations were available from *Yohkoh* (Tsuneta et al. 1991; Kosugi et al. 1991). We use these data sets to put new constraints on the dynamics of the coronal features that lead to type II shock formation, and on the shock's propagation through the corona.

Send offprint requests to: K.-L. Klein (Ludwig.klein@obspm.fr)
⋆ *Current address:* Institute of Space & Astronautical Science, 3-1-1 Yoshinodai, Sagamihara, Kanagawa 229-0022, Japan

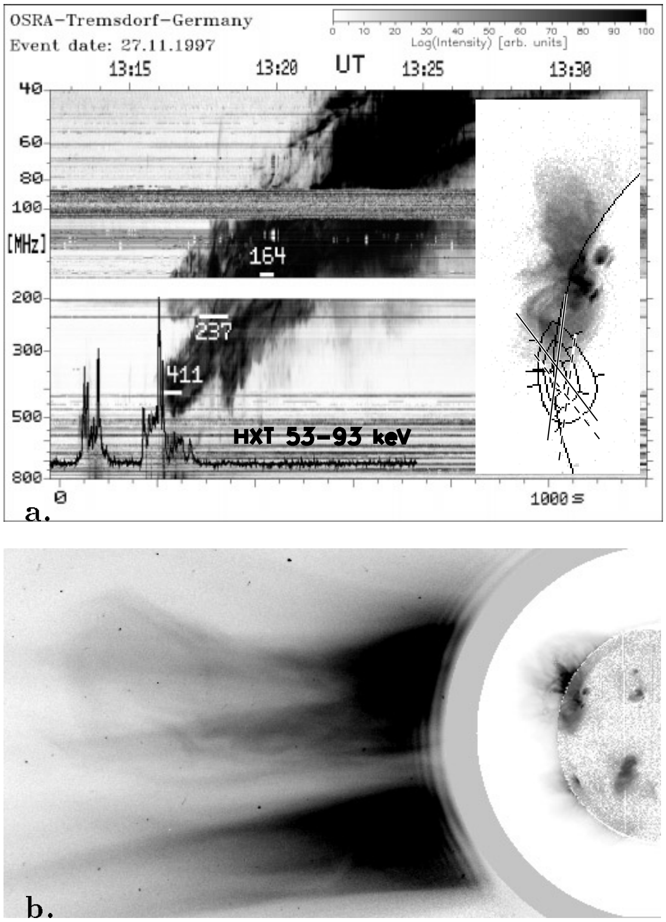

Fig. 1. a Dynamic spectrogram (Tremsdorf Radio spectrograph) and hard X-ray lightcurve (*Yohkoh* HXT) during the 27 November 1997 type II event. Insert: *Yohkoh* SXT negative image of AR 8113 (Al.1 filter) at 1240:36 UT and harmonic type II source during the time intervals indicated by horizontal bars at the appropriate frequencies in the spectrogram: contours of equal brightness at 411 MHz (10, 50, 90% of maximum brightness in the image) and source centroid positions and half widths of the harmonic type II sources at 237 (dashed) and 164 MHz (solid). **b** *Yohkoh* SXT image of (a), superposed on SoHO-LASCO-C1 and C2 images at 1328 and 1330 UT (negative image).

2. Observations

2.1. Radio spectrum and sites of type II emission

The type II burst starts at unusually high frequencies (near 500 MHz, Fig. 1.a). The spectrum does not extend below 7 MHz (WIND homepage, Kaiser 1999, pers. comm.), which means that the emission fades at about (5–10) $R_\odot$ above the photosphere. The type II emission is preceded by impulsive centimetric-to-decimetric and hard X-ray bursts. A 2B Hα flare starts at 1301 UT in active region NOAA 8113 near the north-eastern limb (N16 E63, *Solar Geophys. Data* 645 II) near the bright pre-flare loops seen in soft X-rays (Fig. 1).

The type II harmonic lane intersects all observing frequencies of the NRH. The insert in Fig. 1.a displays, on top of the *Yohkoh* SXT image taken 35 min before the type II burst, the iso-intensity contours of the harmonic type II source at 411 MHz and the centroids and half widths of the sources at 237 and 164 MHz during the time intervals indicated by horizontal bars at the appropriate frequency of the spectrogram (Fig. 1.a). The source centroids and half widths were determined by fitting gaussians to the scans taken with the east-west and north-south branches of the NRH. The type II emission starts south of the flaring active region. The sources are superposed upon each other; they are non-radially aligned along an axis close to the line of sight. We cannot analyze the relative source location in detail, since at the time of observation the accuracy of positioning is limited by the broad beam of the NRH and by ionospheric refraction.

2.2. Evolution of coronal structures and the origin of the type II shock

The type II burst occurs within an evolving environment, both within the underlying active region and on larger scales, as shown by the daily movies of the SoHO-LASCO coronograph (LASCO homepage, Schwenn 1998, pers. comm.). In this section we describe first the global coronal evolution above the eastern solar limb during 27 November 1997, and then present the relationship of the type II burst with the dynamics of flaring active region structures.

Two streamers lie above the eastern limb (Fig. 1.b). In the northern one, which overlies AR 8113, a CME is observed from 1155 UT. It is still in progress at 1330 UT, creating the wavy shape of the northern part of the structure. Both streamers are eventually disrupted by another CME that is visible from 1356 UT at heights >1 $R_\odot$ above the photosphere. The last pre-type II image taken by the C1 coronograph (1244 UT; height range 0.1–2 $R_\odot$ above the photosphere) shows structural changes in the vicinity of the type II source (Schwenn, pers. comm.). The type II emission hence originates within a configuration that is being violently restructured on a very large spatial scale.

A sequence of *Yohkoh* SXT quarter resolution (9.84$''$ pixel size) flare-mode, partial frame images of AR 8113 and its surroundings before and at the onset of the type II burst is displayed in Fig. 2. The first images show diffuse and highly inclined loops extending south-eastward from the inner active region whose emission saturates the detector. Their projected height is $\sim 10^5$ km. In the subsequent images a localized brightening seems to rise along the southern legs of these loops at a projected speed of (770 ± 140) km s^{-1}. It is clearly visible at the border of the saturated region at 1313:42 UT, but shows up in other flare mode images from $\sim$1312:20 UT, near the time of an earlier rise of the hard X-ray emission than shown in Fig. 1.a. When this blob reaches the loop top ($\sim$1315:56 UT), the loop expands and actually seems to be disrupted. A few minutes later, one of the loop legs is clearly visible and appears to straighten out. This straigthened feature persists for several minutes and then fades. Those soft X-ray emitting features from the top and upper parts of the rising loop appear to expand outwards from the Sun, fading as they do so, eventually moving out of the field of view. The first high-frequency signature of the type II burst

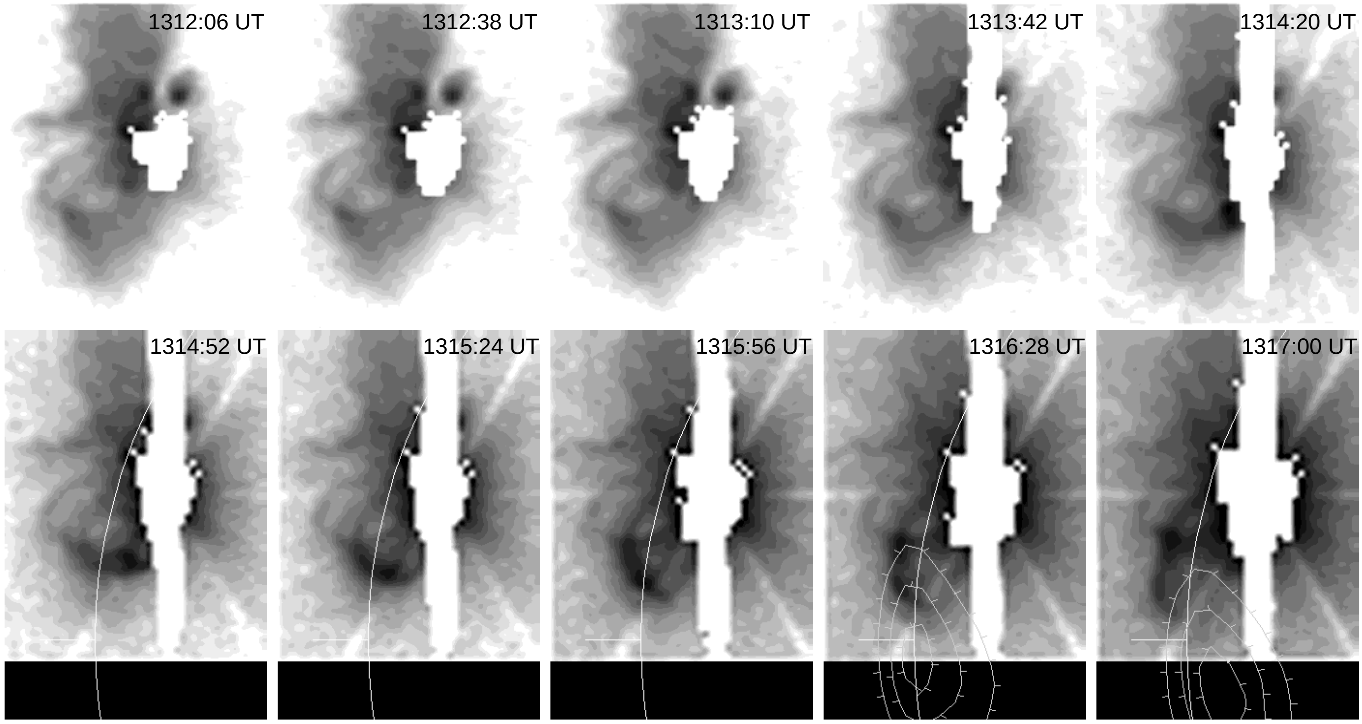

Fig. 2. Time sequence of *Yohkoh* SXT images (AlMg filter) of active region NOAA 8113 and its surroundings prior to and at the onset of the type II burst (negative image: black shading means bright emission). North is up, east to the left. The individual images display a field of $8' \times 10'$. The solar limb is plotted in the bottom panels. The last two panels show the iso-intensity contours of the harmonic type II source at 411 MHz superposed on simultaneous SXT images. The brightest X-ray emission from the flare is saturated and was deleted from the images (bright vertical structure in the *Yohkoh* SXT images). The white star-shaped pattern is an instrumental artifact.

becomes visible near the time of disruption, and just above the loop top (in projection). Two neighboring, but distinct sources are successively observed at 411 MHz, lasting 10 to 20 s each (cf. the superposition on the simultaneous SXT images in the two last panels of Fig. 2). They move eastward, i.e. in the direction of the straightening expanding loop leg, at a projected speed of 1400 km s^{-1}.

The speed of the type II exciter can be derived from the drift rate in the dynamic spectrogram, by use of a model distribution of the thermal electron density along the trajectory. Given the observed non radial propagation, both the gravitational and the magnetic structuring of the coronal plasma must be considered in the density model. If the electron density decreases exponentially with scale height H along the trajectory, the exciter speed is $v_{\rm exc} = \frac{2H}{\nu}\frac{\Delta\nu}{\Delta t} \simeq 970\frac{H}{10^5 {\rm km}} {\rm km\ s}^{-1}$, where $\Delta\nu/\Delta t$ is the frequency drift rate at frequency ν. This is broadly consistent with the estimated speed of the X-ray blob.

3. Discussion

The timing and location of the type II onset with respect to the X-ray features suggest that the origin of the type II burst is closely related to the dynamics of the plasma on spatial scales of active region loops (size $\sim 10^5$ km). The estimated speed of the X-ray blob makes it a plausible driver of a fast shock in the corona. Since the type II source lies above the disrupted X-ray loops and starts in close time coincidence with the disruption, the shock formation seems to be directly related to the disruption of the loop. The soft X-ray signature of the driver persists after the onset of the type II burst. This suggests that intially the type II emission is associated with a driven shock. We cannot decide from the available data if and at which time the energy supply from the driver is turned off so that subsequently the type II shock may become a blast wave.

We conclude a posteriori that a similar case was reported on 27 September 1993 by Klassen et al. (1999; their Fig. 4). In both cases the type II emission starts above an evolving loop, which is seen side-on in the 27 September event, and in projection on the disk on 27 November. Detailed inspection of the *Yohkoh* data on 27 September 1993 suggests that the loop follows a similar evolution to the event discussed in the present paper (Nitta 1998, pers. comm.). A comparable relative position of a presumed type II source (there was no overlap between the frequencies of the imaging and spectral observations) with respect to a rapidly rising X-ray structure was reported by Gopalswamy et al. (1997).

The X-ray blob is reminiscent of the "plasmoids" analyzed by Ohyama & Shibata (1997; 1998), both by its shape and its early onset with respect to the main hard X-ray peak. But its trajectory is clearly curved, following the pre-existing large-scale loops, and its projected speed is higher (770 km s^{-1}, as compared to 200 to 500 km s^{-1}). No type II bursts were observed by the Tremsdorf spectrograph for the events examined by Ohyama & Shibata.

The alignment of the type II sources at different frequencies demonstrates a strongly non-radial propagation of the type II exciter. Non-radial alignment of type II sources has been discussed before (e.g. Nelson & Robinson 1975; Gergely et al. 1983; Stewart 1984; Aurass et al. 1998; Klassen et al. 1999). Among the explanations invoked were the preferential acceleration of electrons in restricted regions of the shock front (e.g. the quasi-perpendicular regime, Steinolfson 1984) and the refraction of the shock wave into regions of low Alfvén speed (Uchida 1974). The present work suggests that the motion of the driver and the magnetic environment where the type II burst occurs may play a role (cf. also Aurass et al. 1998). In the high-frequency range, i.e. close to the place where the shock is generated, the driver seems to impose the site of the first radiative signature of the shock and the direction of propagation.

Acknowledgements. The authors are indebted to J.-P. Delaboudinière (SoHO-EIT) and R. Schwenn (SoHO-LASCO) for generous data supply and helpful comments. We acknowledge discussions with A. Klassen, A. Mangeney, Z. Mouradian and N. Nitta. The Nançay Radio Observatory is funded by the French Ministry of Education, CNRS, and the Région Centre. The *Yohkoh* mission is a project of the Institute of Space and Astronautical Science (ISAS) of Japan. It is funded by ISAS, NASA, and the UK Particle Physics and Astronomy Research Council (PPARC). J.I.K. received support from PPARC.

References

Aurass H., 1997. In: Trottet G. (ed.) Lecture Notes in Physics 483, Coronal Physics from Radio and Space Observations. Springer, Berlin, p. 135
Aurass H., Hofmann A., Urbarz H.-W., 1998, A&A 334, 289
Dryer M., 1981. In: Rosenbauer H. (ed.) Solar Wind Four. Report MPAE-W-100-81-31, 199
Dryer M., 1982, Space Sci. Rev. 33, 233
Gergely T.E., Kundu M.R., Hildner E., 1983, ApJ 268, 403
Gopalswamy N., Kundu M.R., 1995. In: Benz A. O., Krüger A. (eds.) Lecture Notes in Physics 444, Coronal Magnetic Energy Releases. Springer, Berlin, p. 223
Gopalswamy N., Kaiser M.L., Lepping R.P., et al., 1998, JGR 103, 307
Gopalswamy N., Kundu M.R., Manoharan P.K., et al., 1997, ApJ 486, 1036
Hundhausen A.J. 1985, Some macroscopic properties of shock waves in the heliosphere. In: Stone R.G., Tsurutani B.T. (eds.) Geophys. Mon. Ser. 34, Collisionless Shocks in the Heliosphere: A Tutorial Review. AGU, Washington DC, p. 37
Kerdraon A., Delouis J.M., 1997. In: Trottet G. (ed.) Lecture Notes in Physics 483, Coronal Physics from Radio and Space Observations. Springer, Berlin, p. 192
Klassen A., Aurass H., Klein K.-L., et al., 1999, A&A 343, 287
Klein K.-L., Klassen A., Aurass H., LASCO Consortium, 1997. In: The Corona and Solar Wind near Minimum Activity, ESA SP-404, 461
Kosugi T., Makishima K., Murakami T., et al., 1991, Solar Phys. 136, 17
Mann G., 1995. In: Benz A. O., Krüger A. (eds.) Lecture Notes in Physics 444, Coronal Magnetic Energy Releases. Springer, Berlin, p. 183
Mann G., Aurass H., Voigt W., Paschke J., 1992. In: Coronal Streamers, Coronal Loops and Coronal and Solar Wind Composition. ESA SP-348, 129
Nelson G.S., Melrose D., 1985, Type II bursts. In: McLean D.J., Labrum N.R. (eds.) Solar Radiophysics. Cambridge University Press, Cambridge, UK, p. 333
Nelson G.J., Robinson R.D., 1975, PASA 2, 370
Ohyama M., Shibata K., 1997, PASJ 49, 249
Ohyama M., Shibata K., 1998, ApJ 499, 934
Steinolfson R.S., 1984, Solar Phys. 94, 193
Steinolfson R.S., 1985, Theories of shock formation in the solar atmosphere. In: Tsurutani B.T., Stone R.G. (eds.) Geophys. Mon. Ser. 35, Collisionless Shocks in the Heliosphere: Reviews of Current Research. AGU, Washington DC, p. 1
Stewart R.T., 1984, Solar Phys. 94, 379
Tsuneta S., Acton L., Bruner M., et al., 1991, Solar Phys. 136, 37
Uchida Y., 1974, Solar Phys. 39, 431
Wagner W.J., MacQueen R.M., 1983, A&A 120, 136